Aquat. Living Resour. 13 (2000) 283–290

S0990744000010731/FLA

Correcting for position-related bias in estimates of the acoustic backscattering cross-section

Steven J. Fleischman*, Deborah L. Burwen

Division of Sport Fish, Alaska Department of Fish and Game, 333 Raspberry Road, Anchorage, AK 99518-1599, USA

Accepted 11 April 2000

Abstract – Under low signal-to-noise conditions, measurements of the acoustic backscattering cross-section σ_{bs} depend upon the position of the target in the beam. Split- and dual-beam measurements of σ_{bs} increase as the target moves away from the acoustic axis, leading to substantial overestimates of acoustic size for off-axis targets. We show how this phenomenon can be largely explained by measurement error in split-beam estimates of position, and by the effect of a minimum voltage threshold. We demonstrate a two-step correction to remove most of the bias. First, smoothed estimates of position are used to obtain an improved estimate of the beam directivity effect for each echo. Second, the statistical bias induced by the minimum voltage threshold is estimated and subtracted. © 2000 Ifremer/CNRS/INRA/IRD/Cemagref/Éditions scientifiques et médicales Elsevier SAS

target strength / hydroacoustics / measurement error / threshold-induced bias / split beam sonar

Résumé – Correction du biais lié au positionnement dans l'estimation acoustique des sections diffusantes. Dans les conditions de signaux de faible amplitude, les mesures de sections diffusantes σ_{bs} dépendent de la position de la cible dans le faisceau du sondeur. Les valeurs de σ_{bs}, mesurées avec un sondeur à faisceaux concentriques et à faisceaux partagés, augmentent lorsque la cible s'éloigne de l'axe acoustique, conduisant à une surestimation acoustique des cibles hors de l'axe. Nous montrons comment ce phénomène peut être largement expliqué par des mesures d'erreur dans l'estimation de la position, et par l'effet d'un seuil de voltage minimum. Nous établissons et démontrons une correction à deux étapes pour annuler l'essentiel du biais. Tout d'abord, des estimations lissées de la position sont utilisées pour obtenir une estimation améliorée de l'effet de directivité du faisceau pour chaque écho. Ensuite, le biais statistiquement induit par le seuil de voltage minimal est estimé et soustrait. © 2000 Ifremer/CNRS/INRA/IRD/Cemagref/Éditions scientifiques et médicales Elsevier SAS

indice de réflexion / hydroacoustique / mesure d'erreur / effet seuil / sondeur à faisceaux partagés

1. INTRODUCTION

Accurate estimation of the acoustic backscattering cross-section (σ_{bs}) is essential for many fisheries acoustic applications (MacLennan and Simmonds, 1992). However, split- and dual-beam measurements of σ_{bs} depend upon the position of the target in the beam under low signal-to-noise conditions. Measurements of σ_{bs} commonly increase as the target moves away from the acoustic axis, leading to a positive bias in estimates of σ_{bs} for off-axis targets.

This paper addresses position-related bias in split-beam sonar systems. First, we introduce notation and illustrate the problem, using data from a side-looking split-beam sonar in the Kenai River, Alaska. Then we describe a simple mechanism by which measurement error in split-beam estimates of position contributes to the observed bias. We use simulation to show how measurement error, combined with the statistical bias introduced by the use of a voltage threshold, can cause substantial overestimates of σ_{bs} for off-axis targets. We demonstrate how the problem can be greatly reduced by using smoothed estimates of position. Finally, we propose a straightforward correction for threshold-

*Correspondence and reprints.
E-mail address: steve_fleischman@fishgame.state.ak.us (S.J. Fleischman).

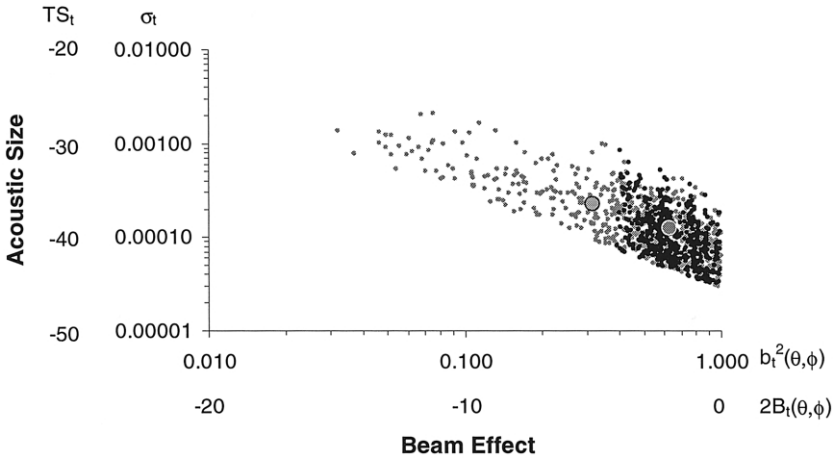

Figure 1. Backscattering cross section versus beam effect for 200 kHz split-beam echoes from a 38.1 mm standard sphere, before (small shaded symbols) and after (small solid symbols) correction for angle measurement error using a local polynomial regression smoother. The target strength estimate (large symbols) changed from –36.5 dB to –39.1 dB after correction for measurement error bias.

induced bias, which is valid when the target echo amplitudes can be described by a Rayleigh distribution.

1.1. Notation

For the remainder of this paper we denote the acoustic backscattering cross-section as σ, rather than σ_{bs}, to avoid the confusion of multiple subscripts. For each echo *t*, σ is estimated by

$$\sigma_t = \frac{e_t^2}{k b_t^2(\theta, \phi)} \quad (1)$$

where e_t is the observed maximum echo amplitude (in volts), k is the overall system gain for an echo sounder with 40 log R + 2 α R time-varied gain, and $b_t^2(\theta, \phi)$ is the 'beam effect', the two-way transducer directional sensitivity as a function of angles θ and ϕ in the horizontal and vertical planes, respectively. The beam effect b^2 is equivalent to b^4 of MacLennan and Simmonds (1992:15) and D^4 of Medwin and Clay (1998).

For a given tracked target, σ is estimated by averaging σ_t over all n echoes:

$$\hat{\sigma} = \frac{1}{n} \sum \sigma_t \quad (2)$$

It is often convenient to express equation (1) in decibel (dB) units:

$$TS_t = 10 \log (\sigma_t) = 20 \log (e_t) - 10 \log (k) - 2B_t(\theta, \phi) \quad (3)$$

where $2B_t(\theta, \phi) = 10 \log (b_t^2(\theta, \phi))$ is the beam effect expressed in decibels. Target strength was estimated by

$$TS = 10 \log (\hat{\sigma}) \quad (4)$$

All logarithms use the base 10. See the axes of *figure 1* to view the correspondence between σ_t and TS_t, and between $b_t^2(\theta, \phi)$ and $2B_t(\theta, \phi)$.

1.2. The problem

Measurements of σ_t often increase with observed distance from the acoustic axis. For example, *figure 1* (small shaded symbols) shows 577 echoes measured from a standard sphere at 13 m horizontal range in the Kenai River. The target was deployed from a boat, which was subject to moderate movement by the river current. Consequently, the target was not stationary in the beam during data acquisition. A strong negative relationship (r = –0.78, P < 0.0001) is evident between σ_t and $b_t^2(\theta, \phi)$ (both log transformed).

Such findings are typical for fish data as well. For example, fish tracked from the left bank of the Kenai River chinook salmon sonar project in 1998 (Bosch and Burwen, 1999) had a mean correlation of r = –0.72 between (log transformed) σ_t and $b_t^2(\theta, \phi)$. We found similar relationships among fish tethered in front of a split-beam transducer (Burwen and Fleischman, 1998). The apparent dependence of σ_t on target position is counter-intuitive, because σ_t has supposedly already been corrected for beam effect (equation 1). This phenomenon leads to over-estimates of σ for targets located off axis. Mechanisms for this bias will be discussed in detail later in this paper.

2. METHODS

2.1. Data collection

Hydroacoustic data were collected with a Hydroacoustics Technology, Inc. (HTI) Model 240 split-beam echo sounder operating at 200 kHz, and a 2.9° × 10° elliptical-beam transducer aimed horizontally across the river. Pulses were 0.2 ms in duration. All measure-

ments were made in freshwater at short ranges, and no correction was made for attenuation due to absorption. Time-varied gain was 40 log(range). Reciprocity calibrations were performed with a standard transducer in April 1998, and the beam effect was mapped and approximated as a fourth-order polynomial of angles θ and ϕ:

$$10 \log (b^2(\theta, \phi)) = 0.0005 - 0.0003\,\theta - 0.2136\,\theta^2 + 0.0049\,\theta^3 - 0.0001\,\theta^4 + 0.0011\,\phi - 2.4835\,\phi^2 + 0.0172\,\phi^3 - 0.1855\,\phi^4 \quad (5)$$

Hydroacoustic data on a tungsten carbide sphere (38.1 mm diameter, theoretic TS = –39.5 dB) were collected on June 12, 1998 in the Kenai River, Alaska. Additional data were collected on fish, composed primarily of chinook and sockeye salmon, migrating up the Kenai River during May–August 1998. Minimum voltage thresholds, set just above maximum background noise, were 0.2 V (equivalent to a –45 dB target on axis) for the standard target data, and 0.66 V (–35 dB) for the fish data. Pulses were transmitted at a rate of 11 s^{-1} for the standard target data and 16 s^{-1} for the fish data. See Bosch and Burwen (1999) for additional details about the sonar system and its deployment.

We estimated the error in split-beam angle measurements by applying a smoother to time series of θ and ϕ (see the results section), and then using the mean-squared errors of the smoother as estimates of measurement error variances s^2_ϕ and s^2_ϕ.

2.2. Simulations

We assumed Rayleigh-distributed echo amplitudes, equivalent to exponentially-distributed σ_t. Thus we generated 50 000 exponentially-distributed variates with mean $\hat{\sigma}$ = 0.0251 (TS = –26 dB), then multiplied by the system gain and the true beam effect to simulate hypothetical squared echo amplitudes (equation 1 solved for e_t^2). True angular position coordinates θ and ϕ were modified by adding independent gaussian measurement error with mean 0 and standard deviations s_θ and s_ϕ. The new (corrupted) estimates of $b_t^2(\theta, \phi)$ and σ_t were obtained using equations 5 and 1. System parameters for the simulation were chosen to match those of our hydroacoustic equipment, described above (overall gain k = 1 265, beam pattern as described by equation 5).

3. RESULTS

3.1. Effect of position measurement error

We found that much of the observed dependence between σ_t and $b_t^2(\theta, \phi)$ can be explained by measurement error in estimates of position. Split-beam sonar measures phase differences to estimate target position. In the presence of noise, phase measurements are corrupted (Ehrenberg and Torkelson, 1996), introducing error into estimates of θ and ϕ. For instance, *figure 2* shows the time series of θ and ϕ position estimates from the standard target data in *figure 1*. Ping-to-ping changes in position estimates are caused not only by movement of the target (low frequency variability in *figure 2*), but also by measurement error (high frequency jitter).

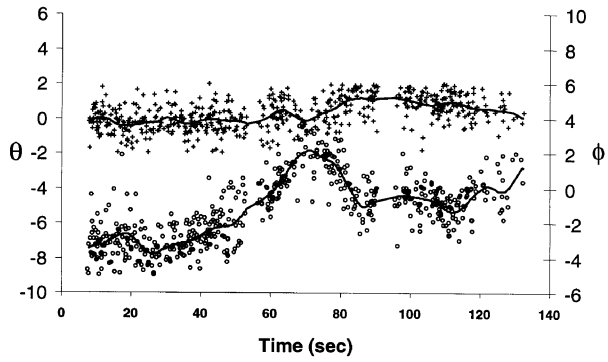

Figure 2. Time series of θ (circles) and ϕ (plus symbols) for 200 kHz split-beam data from a 38.1 mm standard sphere, overlaid by smoothed position estimates (lines) from a local polynomial regression procedure.

Measurement error in the θ and ϕ dimensions causes error in the estimate of the beam effect $b_t^2(\theta, \phi)$ (equation 5). Furthermore, any error in $b_t^2(\theta, \phi)$ results in an inverse error in σ_t. For instance, if $b_t^2(\theta, \phi)$ is *over*estimated by a factor of 2, σ_t is *under*estimated by one-half, and vice versa (equation 1). Expressed in decibels, if $2B(\theta, \phi) = 10 \log (b_t^2(\theta, \phi))$ is overestimated by x dB, $TS_t = 10 \log (\sigma_t)$ is underestimated by x dB, and vice versa (equation 3). Therefore any θ, ϕ measurement error causes a negative one-to-one correspondence of TS_t and $2B(\theta, \phi)$. *Figure 3* shows simulated data from a stationary target subject to increasing θ, ϕ measurement error. With sufficiently large measurement error, the result is a strong negative relationship like that exhibited in *figure 1*.

3.2. Bias in $\hat{\sigma}$

Measurement error in θ and ϕ therefore explains the observed dependence of σ_t and $b_t^2(\theta, \phi)$. More importantly, angle measurement error causes estimates of σ to be biased high, as explained below.

First, it is convenient to rewrite equation (1) as follows:

$$\sigma_t = k^{-1} e_t^2 F_B \quad (6)$$

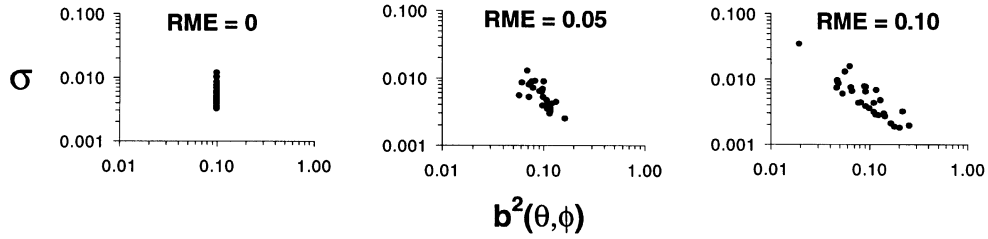

Figure 3. Backscattering cross section versus beam effect for simulated data from a stationary target subject to increasing levels of relative measurement error (RME) in angular position estimates. Simulations were done with a –27 dB target and a –35 dB threshold. RME is defined as the measurement error standard deviation divided by the half power beam width.

where $F_B = \frac{1}{b_t^2(\theta, \phi)}$ is the 'beam correction factor', the inverse of the beam effect.

Figure 4a shows simulated position estimates from an off-axis target on a beam contour plot, where contour lines connect points of equal F_B. Note that the contour lines become closer together (F_B changes more rapidly) with increasing distance from the acoustic axis. The target in *figure 4a* is stationary at $\theta = 3°$ and $\phi = -1.3°$, corresponding to a true beam correction factor of $F_B = 4$. However, since the individual measurements of θ and ϕ are subject to measurement error, so are the estimates of F_B. And because F_B changes more rapidly near the 'edge' of the beam, positive deviations from the true correction factor are generally larger in magnitude than negative deviations. The result is that the distribution of F_B is skewed to the right, and its mean exceeds the true value (*figure 4b*). Since σ_t is a function of F_B (equation 6), the mean of σ_t (which is our estimate of the acoustic backscattering cross-section) is also biased high.

This 'measurement-error bias' depends on position in the beam. Near the axis, the beam pattern is flat, so $\theta\phi$ measurement error does not generate much variability in the estimate of $b^2(\theta, \phi)$ and the bias is minimal. Away from the axis, $b^{-2}(\theta, \phi)$ is more sensitive to position (and errors in position), and the bias is greater.

Estimates of σ are also influenced by threshold-induced bias (Weimer and Ehrenberg, 1975), whereby selective exclusion (censoring) of small-amplitude echoes by a minimum voltage threshold causes a positive statistical bias. Like the measurement-error bias, threshold-induced bias becomes more pronounced with distance off-axis. For example, the data in *figure 1* were subject to a minimum voltage threshold of 0.2 V. That is, echoes with amplitudes less than 0.2 V were censored to minimize acquisition of noise. With this system (gain $k = 1\,265$), and for a target located on axis ($b_t^2(\theta, \phi) = 1$), this voltage threshold excludes echoes with backscattering cross section less than $\sigma_t = 0.2^2 \times 1\,265^{-1} = 0.000032$ (equation 1) or $TS = -45$ dB (equation 3). However, for a target located off axis, say at $b_t^2(\theta, \phi) = 0.5$, the same 0.2 V threshold excludes echoes with $\sigma_t < 0.000064$ ($TS < -42$ dB). Similarly, at $b_t^2(\theta, \phi) = 0.25$, it excludes echoes with $\sigma_t < 0.000128$ ($TS < -39$ dB). Thus an increasing proportion of returning echoes are left-censored (small echoes rejected) as the target moves off axis, and the bias increases.

Measurement-error bias and threshold-induced bias combine to produce substantial overestimates of σ (*figure 5*). As expected, our simulations show that the magnitude of the bias depends on target position. In addition, the bias depends on the signal-to-threshold ratio (STR), and on the amount of $\theta\phi$ measurement error relative to the width of the beam. When the signal from the target is large relative to the voltage threshold, and when the standard deviation of the measurement error is small relative to the beam width, the bias is minimal (*figure 5*). Generally, one encounters such conditions when the signal-to-noise ratio

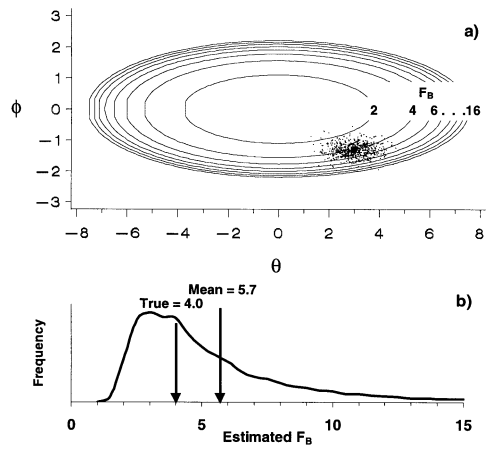

Figure 4. Bias in estimates of σ as a consequence of measurement error in $\theta\phi$ positional estimates: a) contour diagram of beam correction factor $F_B = b^{-2}(\theta\phi)$, with simulated $\theta\phi$ positional data subject to measurement error superimposed; b) resulting distribution and mean of estimated F_B.

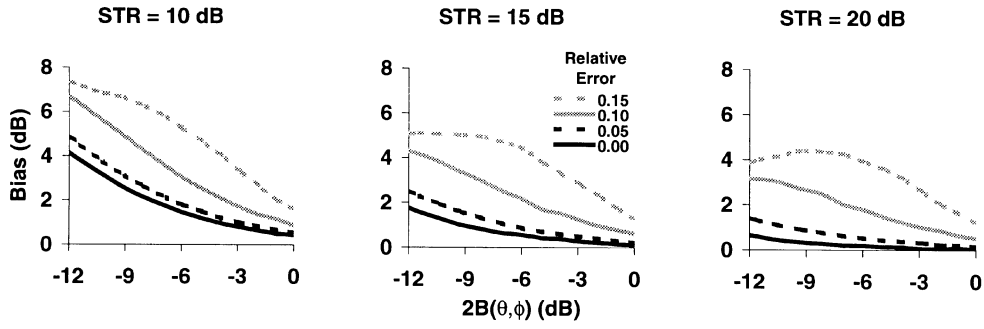

Figure 5. Bias ($10 \log (\hat{\sigma}/\sigma)$) versus beam effect for four levels of relative measurement error (RME) and three signal-to-threshold ratios (STR). RME is defined as the measurement error standard deviation divided by the half power beam width. STR is defined as the difference between target strength and $10 \log e_T^2 k^{-1}$, where e_T is the voltage threshold.

(SNR) is high. Under low SNR (high noise or volume reverberation), higher thresholds are required and the amount of measurement error generally increases, both of which lead to greater bias (*figure 5*). Such conditions are the norm in riverine acoustic applications. In our application, STR is usually 10–15 dB and measurement error standard deviations range between 10% and 15% of beam width. Under these conditions, our simulations predict that our estimates of *TS* will be 1–2 dB too high for on-axis targets and 2–6 dB too high for targets located at the half-power point ($2B(\theta, \phi) = -6$ dB, *figure 5*).

Our simulations in *figure 5* were conducted with a beam-angle threshold of –24 dB. That is, any echoes for which the estimated beam effect $2B(\theta,\phi)$ was less than –24 dB were censored. Increasing the beam angle threshold can reduce the magnitude of the bias (*figure 6*). Unfortunately this solution is not entirely satisfactory, for several reasons. First, the magnitude of the bias remains position-dependent, even after applying the beam angle threshold. Second, the direction of the bias can change. For example, with a beam effect threshold of –6 dB, targets positioned more than 5 dB off axis are subject to a negative bias (*TS* will be underestimated, *figure 6*). Finally, censoring echoes far from the axis reduces the number of echoes available to estimate σ. We propose a more robust solution below, one which does not have the above disadvantages.

3.3. Smoothed position estimates to reduce bias

The bias described above is partially due to the nonlinear transformation from θ (and ϕ) to F_B (*figure 7*). Symmetric error in θ or ϕ results in asymmetric error in F_B. Our solution for reducing the bias is to exploit the information from multiple echoes to improve the estimates of position *before* doing the nonlinear transformation to F_B. As a simple example, if one knew the target to be stationary, one could use the mean position estimates across all echoes $\bar{\theta}$ and $\bar{\phi}$ to estimate one beam correction factor $\hat{F}_B = b^{-2}(\bar{\theta}, \bar{\phi})$, then use this single (and more precise) estimate in the estimate of σ (*figure 7*).

For a moving target, this strategy can be generalized as follows: for a given echo, exploit the information from neighboring echoes to obtain a more precise estimate of position, then convert to F_B. That is, find:

$$\hat{\theta}_t = g_\theta (\theta_{t-\lambda}, \theta_{t-\lambda+1}, ..., \theta_{t+\lambda-1}, \theta_{t+\lambda}) \quad (7)$$

$$\hat{\phi}_t = g_\phi (\phi_{t-\lambda}, \phi_{t-\lambda+1}, ..., \phi_{t+\lambda-1}, \phi_{t+\lambda}) \quad (8)$$

where $g_\theta(\ )$ and $g_\phi(\ )$ are smoothing functions of θ and ϕ, respectively, within λ pings of t.

The improved estimates of position can then be used to generate more precise estimates of the beam effect $\hat{b}^2(\hat{\theta}, \hat{\phi})$, using the appropriate transformation, such as equation 5.

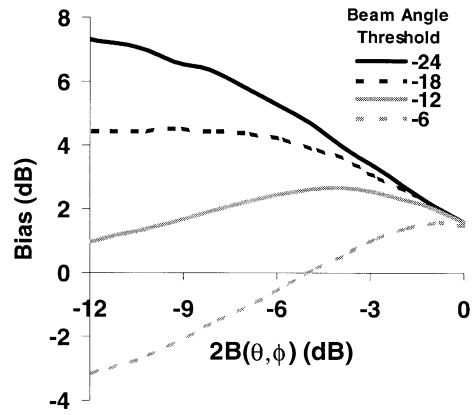

Figure 6. Simulated effect of a beam angle threshold on position-related bias ($10 \log (\hat{\sigma}/\sigma)$) versus beam effect. All simulations were conducted with 10 dB signal-to-threshold ratio and 15% relative measurement error (top line in graph is thus the same as the top left line in *figure 5*). Additional lines represent the effect of raising the beam angle threshold; e.g., the dashed gray line is the bias to be expected if all echoes with estimated beam effect $2B(\theta\phi)$ less than –6 dB were censored.

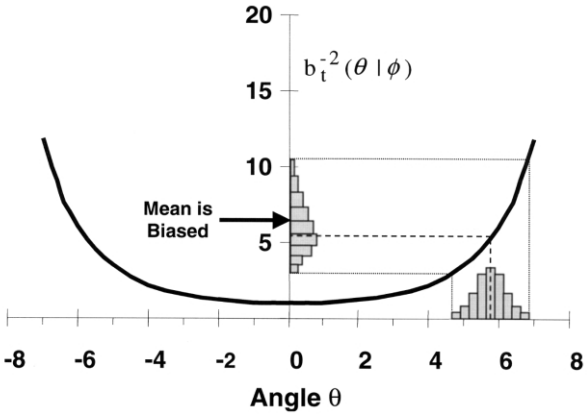

Figure 7. Exploiting the information from multiple echoes to reduce bias due to angle measurement error. Solid line is the beam correction factor $F_B = b^{-2}(\theta\phi)$ as a function of angle θ with angle $\phi = 0$. Because the transformation is nonlinear, symmetric error in estimating θ results in asymmetric error in $\boldsymbol{F}_B$, and bias results. A simple and effective way to reduce the bias is to compute the mean of θ from multiple echoes, *then* convert to F_B (dashed lines).

Finally, σ is re-estimated for each echo, using the improved estimate of beam pattern:

$$\hat{\sigma}_t = e_t^2 \, k^{-1} \, \hat{b}_t^{-2}(\hat{\theta}, \hat{\phi}) \qquad (9)$$

There are several possible choices for the smoothing function g, including parametric polynomial regression and nonparametric smoothing splines, kernal smoothers, or local regression (loess) smoothers.

We applied a nonparametric local polynomial fixed-bandwidth smoother (Cleveland, 1993, SAS Institute, 1995) to the standard target data (*figure 2*); with bandwidth $\lambda = 100$ (equivalent to about 9 s), tri-cube weighting, and 128 intervals. This smoother fits a quadratic regression between the position estimates and time at each interval, and uses the regression predicted values as the smoothed estimates of position. It was applied, independently, to the estimates of θ, then ϕ. The procedure removed virtually all of the 'jitter' from the position estimates (*figure 2*). The resulting corrected estimates of σ_t and $b_t^2(\theta, \phi)$ are less correlated ($r = 0.48$) than the original data ($r = 0.78$) (*figure 1*). Moreover, the corrected target strength (–39.1 dB) is 2.6 dB less than that estimated from the original, unsmoothed data (–36.5 dB), due to the reduction in bias (*figure 1*). The theoretical *TS* for a 38.1 mm sphere with 200 kHz frequency in fresh water is –39.5 dB (MacLennan and Simmonds, 1992). Other smoothers yielded results very similar to these (not shown).

We applied a similar smoother to hydroacoustic data collected from migrating salmon in the Kenai River in 1998. After correction for measurement error, the formerly strong dependence between acoustic size and position was much reduced (not shown), as were estimates of σ. For the six fish shown in *figure 8* bias was reduced between 0.9 and 2.8 dB (compare large shaded symbols with and without crosshairs).

3.4. Correction for threshold-induced bias

After implementing the smoothing procedure described above, estimates of σ are still subject to threshold-induced bias. We propose the following correction to remove it. The correction is valid if the echo amplitudes are Rayleigh-distributed, which generally holds true if the ratio of target length to wavelength is greater than 20 (Clay and Heist, 1984). At a carrier frequency of 200 kHz, the wavelength equals 1 500 m·s^{-1}/200 000 Hz = 0.0075 m, so targets greater than 7.5 mm × 20 = 15 cm in length are likely to have Rayleigh-distributed amplitudes. Clearly the fish in *figure 8* meet this condition (Kenai R. salmon range from 40 to 110 cm in length), but the standard target (*figure 1*) does not.

If the echo amplitudes e_t are Rayleigh-distributed, then e_t^2 and σ_t are exponentially distributed (Evans et al., 1993). Assuming for the moment that a target is stationary on the acoustic axis, then applying a voltage threshold of e_T is equivalent to applying a backscattering cross section threshold of $\sigma_T = e_T^2 \, k^{-1}$ (equation 1). Left censoring σ_t, such that all echoes with $\sigma_t < \sigma_T$ are not observed, biases σ high by an amount β_T. Conveniently, if σ_t has an exponential distribution, the bias β_T is equal to the threshold σ_T (see Appendix). Since the bias is known, one can correct for it by subtracting $\sigma_T = e_T^2 \, k^{-1}$ from each σ_t.

Generalizing to an echo originating from a target located off-axis, the effective threshold is $\sigma_T = e_T^2 \, k^{-1} \, b_t^{-2}(\theta, \phi)$, and the appropriate corrected estimate of σ_t is:

$$\sigma_t' = \sigma_t - e_T^2 \, k^{-1} \, b_t^{-2}(\theta, \phi) \qquad (10)$$

This correction can be quite large for targets which barely exceed the voltage threshold, or for targets far from the acoustic axis. Note that the mean of σ_t' is an unbiased estimate of σ only when $b_t^{-2}(\theta, \phi)$ is estimated accurately, so the correction for $\theta\phi$ measurement error should be applied (Equations 7–9) *before* correcting for threshold-induced bias.

Figure 8 shows the combined effect of correcting for measurement-error bias and threshold-induced bias. Virtually all of the dependence between acoustic size and position is removed (mean correlation $r = –0.12$), and bias is reduced between 1.9 and 6.0 dB.

4. DISCUSSION

Our findings are important for any split-beam application with a low signal-to-noise ratio (SNR) which produces estimates of σ or *TS*. Under high SNRs (25–30 dB or more), split-beam estimates of σ are

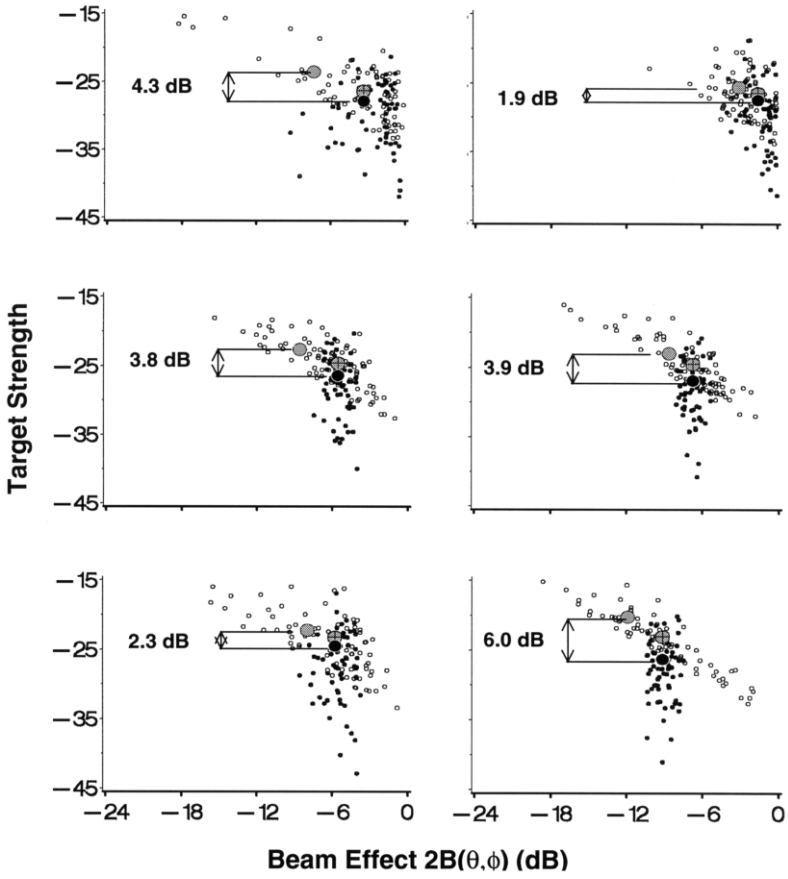

Figure 8. Backscattering cross section versus beam effect for 200 kHz split-beam data from six migrating salmon in the Kenai River, before (small open symbols) and after (small solid symbols) correction for position-related bias. Large symbols represent point estimates (1) before any correction (shaded), (2) after correction for $\theta\phi$ measurement error (shaded with crosshairs), and (3) after further correction for threshold-induced bias (solid). The resulting total reduction in estimated target strength after applying both corrections is shown.

virtually unbiased (Ehrenberg, 1979; Ehrenberg and Torkelson, 1996). As SNR decreases, angle measurement error increases and voltage thresholds must be raised to eliminate noise, both of which cause bias to increase.

Application of the corrections described above are particularly crucial for side-looking hydroacoustic applications in rivers, where high reverberation levels result in low SNR's, and where fish often migrate near the bottom and thus toward the periphery of the beam. In such applications, the distribution of targets in the beam is very sensitive to transducer aim. On the Kenai River, we often see radical changes (> 3 dB) in the target strength distribution of tracked fish after vertically adjusting the aim only a small fraction of a degree. Such changes in aim have the potential to completely swamp any differences in *TS* due to changes in the size distribution of fish. The corrections described in this paper greatly reduce the confounding influence of aim on *TS*.

Finally, low SNR may also lead to other biases in split-beam measurements which depend upon position in the beam. For instance, the relative additive effect of noise on echo amplitude increases with distance off-axis. Also, Kieser et al. (2000) have observed that, under low SNR, split-beam estimates of position are biased toward the acoustic axis, thereby causing a negative bias in σ for off-axis targets. These additional considerations will be addressed in future work.

Acknowledgements. We thank John Ehrenberg, Robert Kieser, and Tim Mulligan for many fruitful discussions and for their comments on the manuscript. Two anonymous reviewers provided insightful comments and helpful suggestions. Dan Bosch and Mark Jensen collected the data presented herein. This project was partially funded by the U.S. Fish and Wildlife Service through the Federal Aid in Fish Restoration Act under projects F-10-13 and F-10-14, job S-2-28.

Appendix

If σ has an exponential distribution, its pdf and cdf are as follows:

$$f(\sigma) = \frac{1}{\bar{\sigma}} e^{-\frac{\sigma}{\bar{\sigma}}} \quad F(\sigma) = 1 - e^{-\frac{\sigma}{\bar{\sigma}}}$$

where $\bar{\sigma}$ is the mean of σ.

When an exponential variate σ is left-censored, say at σ_T, only those values of σ greater than σ_T are observed. Its mean $E[\sigma_{obs}]$ is then biased high by the following amount:

$$\beta_T = E[\sigma_{obs}] - E[\sigma]$$

$$= \frac{\int_{\sigma_T}^{\infty} \sigma f(\sigma)\, d\sigma}{\int_{\sigma_T}^{\infty} f(\sigma)\, d\sigma} - \bar{\sigma}$$

$$= \frac{\int_{\sigma_T}^{\infty} \sigma \frac{1}{\bar{\sigma}} e^{-\frac{\sigma}{\bar{\sigma}}}\, d\sigma}{1 - (1 - e^{-\frac{\sigma_T}{\bar{\sigma}}})} - \bar{\sigma} \quad \begin{array}{l}(\text{substitute pdf into numerator,}\\ \text{cdf into denominator})\end{array}$$

$$= \frac{-(\sigma + \bar{\sigma})\, e^{-\frac{\sigma}{\bar{\sigma}}}\Big|_{\sigma_T}^{\infty}}{e^{-\frac{\sigma_T}{\bar{\sigma}}}} - \bar{\sigma} \quad (\text{integration by parts})$$

$$= \frac{0 - (-\sigma_T - \bar{\sigma})\, e^{-\frac{\sigma_T}{\bar{\sigma}}}}{e^{-\frac{\sigma_T}{\bar{\sigma}}}} - \bar{\sigma}$$

$$= \sigma_T$$

References

Bosch, D., Burwen, D.L., 1999. Estimates of chinook salmon abundance in the Kenai River using split-beam sonar, 1997. Fish. Data Ser. No. 99–3, Alaska Department of Fish and Game, Anchorage, Alaska.

Burwen, D.L., Fleischman, S.J., 1998. Evaluation of side-aspect target strength and pulse width as potential hydroacoustic discriminators of fish species in rivers. Can. J. Fish. Aquat. Sci. 55, 2492–2502.

Clay, C.S., Heist, B.G., 1984. Acoustic scattering by fish – Acoustic models and a two parameter fit. J. Acoust. Soc. Am. 75, 1077–1083.

Cleveland, W., 1993. Visualizing Data. AT& T Bell Laboratories.

Ehrenberg, J.E., 1979. A comparative analysis of in situ methods for directly measuring the acoustic target strength of individual fish. IEEE J. Ocean Engin. 4, 141–152.

Ehrenberg, J.E., Torkelson, T.C., 1996. Application of dual-beam and split-beam target tracking in fisheries acoustics. ICES J. Mar. Sci. 53, 329–334.

Evans, M., Hastings, N., Peacock, B., 1993. Statistical Distributions. John Wiley and Sons, New York.

Kieser, R., Mulligan, T.J., Ehrenberg, J.E., 2000. Observation and explanation of noise-induced split-beam angle measurement errors. Aquat. Living Resour. 13, 275–281.

MacLennan, D.N., Simmonds, E.J., 1992. Fisheries Acoustics. London, Chapman and Hall.

SAS Institute Inc., 1995. SAS/INSIGHT User's Guide, Version 6, 3rd edn. SAS Institute Inc. Cary, NC.

Medwin, H., Clay, C.S., 1998. Fundamentals of Acoustic Oceanography. Academic Press, San Diego.

Weimer, R.T., Ehrenberg, J.E., 1975. Analysis of threshold-induced bias inherent in acoustic scattering cross-section estimates of individual fish. J. Fish. Res. Board Can. 32, 2547–2551.